

pubs.acs.org/synthbio Research Article

Electrogenetic Signal Transmission and Propagation in Coculture to Guide Production of a Small Molecule, Tyrosine

Eric VanArsdale, Juliana Pitzer, Sally Wang, Kristina Stephens, Chen-yu Chen, Gregory F. Payne, and William E. Bentley*



Cite This: https://doi.org/10.1021/acssynbio.1c00522



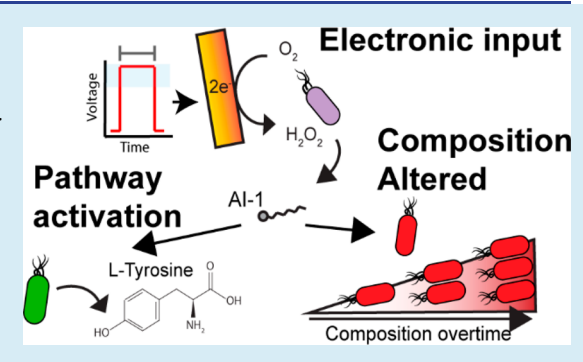
ACCESS I

Metrics & More

Article Recommendations

s Supporting Information

ABSTRACT: There are many strategies to actuate and control genetic circuits, including providing stimuli like exogenous chemical inducers, light, magnetic fields, and even applied voltage, that are orthogonal to metabolic activity. Their use enables actuation of gene expression for the production of small molecules and proteins in many contexts. Additionally, there are a growing number of reports wherein cocultures, consortia, or even complex microbiomes are employed for the production of biologics, taking advantage of an expanded array of biological function. Combining stimuli-responsive engineered cell populations enhances design space but increases complexity. In this work, we co-opt nature's redox networks and electrogenetically route control signals into a consortium of microbial cells engineered to produce a model small molecule, tyrosine. In particular, we show how electronically



programmed short-lived signals (i.e., hydrogen peroxide) can be transformed by one population and propagated into sustained longer-distance signals that, in turn, guide tyrosine production in a second population building on bacterial quorum sensing that coordinates their collective behavior. Two design methodologies are demonstrated. First, we use electrogenetics to transform redox signals into the quorum sensing autoinducer, AI-1, that, in turn, induces a tyrosine biosynthesis pathway transformed into a second population. Second, we use the electrogenetically stimulated AI-1 to actuate expression of *ptsH*, boosting the growth rate of tyrosine-producing cells, augmenting both their number and metabolic activity. In both cases, we show how signal propagation within the coculture helps to ensure tyrosine production. We suggest that this work lays a foundation for employing electrochemical stimuli and engineered cocultures for production of molecular products in biomanufacturing environments.

KEYWORDS: coculture, signal propagation, electrogenetics, quorum sensing

ynthetic biology offers the promise of rationally engineered cells that can be used in cell-based molecular manufacturing or in hybrid biodevices where "programmed" cell function is the desired output (e.g., cell-based biosensors). Many of these systems utilize the unique capacity of biology to catalyze difficult reactions, produce heterologous compounds, or respond to various cues. To be effective, genetic circuits are triggered by a variety of means to ensure proper resource utilization and at the same time limit off-target action. For instance, controlling metabolic flux through interactions with carbon source utilization^{1,2} or by switching carbon flow throughout the various stages of product formation³⁻⁵ has resulted in significant product enhancement. In an analogous manner, cell-based therapeutic devices act on specific cues to both process a patient's molecular data and mediate a therapeutic regimen on-demand.°

At the forefront of these designs is the use of molecular, optical, magnetic, or other switches, each with attractive features for initiating and controlling outcomes. For example, optical genetic switches offer the promise of automated control in specialized optically compliant reactors 10,11 or biomedical

devices. ^{12,13} Magnetic switches offer controlled gene expression deep within a patient's body by targeting engineered cell populations functionalized with nanomaterials. ¹⁴ In these examples, seemingly disparate components are pieced together into a functioning system. In molecular manufacturing applications, there is great interest in appending fractional biosynthesis functions, including components from disparate organisms, into complete synthesis pathways that are assembled into two or more cell types that when cultivated together confer unique advantages for the overall system. ¹⁵ For instance, coculture systems have been assembled such that one cell can catabolize a particular sugar and produce an intermediate while another cell can then turn that intermediate into a useful product. ^{16,17} This general scheme allows each task

Received: October 15, 2021

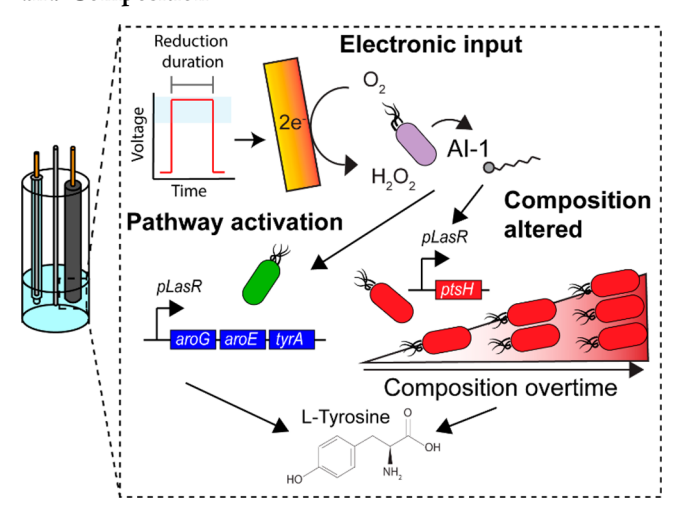


within a design structure to be optimized within an individual cell population, which can then be modularly deployed. ^{18–20} These advantages come at the cost, however, in that system level dynamics, including elements of communication ²¹ and stochasticity can create unforeseen consequences. Controlling subpopulation composition, while offering extra knobs for engineering design, can be challenging, sometimes requiring toxic or burdensome dampening to reduce or eliminate certain subpopulations. ^{22,23} Translating these systems to large volume reactors can also be daunting and unpredictable ^{24,25} making continuous processes infeasible.

Electrogenetic methodologies that link electronically responsive genetic circuits with advanced signal processing and control methodologies may provide a means for addressing these challenges. Electrochemical methods that control biological activity commonly employ inducible promoters²⁶ or voltage-gated channels.⁶ Our group has specifically targeted redox electrogenetic methods,²⁷ which rely on diffusible mediators to carry electrons between an electrode and actuatable cells where redox reactions activate engineered gene circuits. This specific design allows these systems to operate in opaque solutions with little equipment and/or power requirements. These systems also enable unique forms of control, including those that exploit electrochemically imposed gradients of induction²⁸ or "living electrodes" wherein engineered cells are directly attached to electrodes and electrode-generated hydrogen peroxide mediates information transfer to the electrogenetic circuits.²⁹ In this way, a conductive surface, but no chemical additives, are needed for information transfer. Further, by employing electrogenetic circuits that serve to generate bacterial quorum sensing signals, one can propagate communication throughout a coculture.² Note that redox-based electrochemical methodologies are also well-paired with optical techniques, enabling more complex and networked control schemes.³⁰

In the current work, we designed and tested a general electrogenetic control methodology, depicted in Scheme 1, as a means to electronically initiate the synthesis and propagation of quorum sensing (QS) signals that, in turn, regulate small molecule (tyrosine) production. We further show the benefit of a hybrid electrogenetic/QS signaling modality enables the propagated signal to modulate tyrosine production in two ways. In both cases, dissolved oxygen is reductively converted to hydrogen peroxide via the 2-electron oxygen-reduction reaction (ORR)³¹ at a gold electrode and this serves as an initial signal relay. Hydrogen peroxide then permeates nearby "transmitter" cells (Scheme 1, purple cells) activating oxyRbased gene circuits through oxidative interactions with the OxyR cysteine residues³² to generate the bacterial quorum sensing autoinducer-1, N-3-oxo-dodecanoyl-L-homoserine lactone (i.e., AI-1). In this way, the hydrogen peroxide "information" is collected, assessed for concentration, and then converted and conveyed throughout the culture to either of two second populations. In the first case, the AI-1 controls the synthesis of tyrosine by directly stimulating its biosynthesis pathway (Scheme 1, green cells) or, in the second case by stimulating the growth rate of a different population of cells that constitutively produce tyrosine (Scheme 1, red cells). Specifically, in this latter case, the AI-1 activates expression of ptsH, which increases metabolic activity, growth rate, and the fraction of cells constitutively producing tyrosine. Hence, in both cases, the original electronic input is converted to quorum sensing signals that, in turn, modulate tyrosine synthesis in a

Scheme 1. Electronic Control over Coculture Production and Composition a



"Electrochemical information is input via applied voltages and total charge at a gold electrode surface. These "commands", in the form of hydrogen peroxide, are sensed by cells to activate a gene circuit. Referred to as "transmitter" cells, these bacteria interpret the hydrogen peroxide signal, transform it to a quorum sensing signal, and relay the information to other "receiver" cells, ultimately stimulating tyrosine production.

coculture. Cells are engineered to receive, interpret, transmit, and act on molecular stimuli in order to produce tyrosine.

In this work, we sought to address several design challenges relative to information transfer, gene actuation and coculture design. These include understanding how best to generate hydrogen peroxide and how best to convert and transmit its information content to a second population of cells responsible for tyrosine synthesis. Issues such as coculture composition, heterogeneity of signal transmission, and the dynamics of signal generation, propagation, and gene expression all play a role in a system design. Fortuitously, because tyrosine can be measured electrochemically, both the initial transmission signal and the final product measurement can be mediated using common microelectronics devices.

We made a few key observations: (i) We found that the H₂O₂-generating ORR reaction stimulates only a fraction of the actuatable cells within the stirred culture likely due to the localized nature of the reaction. This was in agreement previous modeling predictions of H2O2 generation, distribution, and cell uptake.²⁹ (ii) We found that a transmitterreceiver modality is quite effective. Here, one population transforms the electronic hydrogen peroxide signal into a nonmetabolized biological quorum sensing signal molecule (AI-1) that, in turn, serves as a "second messenger" that is transmitted to a "receiver" population. (iii) We found that a homogeneous and multileveled response can be created even when the transmitter oxyR-gene circuit is best characterized by an ON/Off modality activated in a small fraction of the overall population. (iv) And last, we found that the basic design construct that networks information propagation between electronic and biological forms could function effectively, even when using different genetic circuits that mediate product synthesis. We suggest these attributes make this electronic methodology simple and applicable for both laboratory and biomanufacturing settings.

Table 1. Plasmids

plasmid name	defining features	ref
OxyR-sfGFP	Produces sfGFP in response to hydrogen peroxide; AmpR	29
OxyR-LasI-LAA	Produces the LasI synthase with the LAA ssrA degradation tag in response to hydrogen peroxide; AmpR	29
AI-1-GFPmut3	Produces GFPmut3 in response to the autoinducer-1 species produced by the LasI synthase; AmpR	36
AI-1-tyrosine	Expresses the genes $aroG$, $aroE$, and $tyrA$ in response to the autoinducer-1 species produced by the LasI synthase; $AmpR$	34
pAHL-pstH	Produces the HPr protein of the phospotransferase system in response to the autoinducer-1 species produced by the LasI synthase; $AmpR$	2
ZA-tyrosine	Constitutively expresses the genes aroG, aroE, and tyrA from an uninhibited pLtet0-1 promoter; CmpR	This work
OxyR-LasI-LAA-GFPmut3 (OLG)	Produces both the LasI synthase with the LAA ssrA degradation tag and GFPmut3 in response to hydrogen peroxide; $AmpR$	This work

METHODS

Strains and Materials. All chemicals, unless specified, were purchased from Sigma-Aldrich (St. Louis, Missouri). The minimal media recipe used in this work was described previously. N-3-oxo-dodecanoyl-L-homoserine lactone was purchased from Cayman Chemicals (Ann Arbor, MI). *E. coli* DH5 α (F-, φ 80lacZ Δ M15, Δ (lacZYA argF)U169, recA1, endA1, hsdR17(rK-, mK+), phoA, supE44, λ -, thi-1, gyrA96, relA1, Invitrogen, Carlsbad, CA) was the primary strain used in this work unless otherwise specified. *E. coli* strain O:17 (F-, Δ (*ompT*, *soxRS*, *tyrR*), sup+,) was constructed in a previous work. E. coli strain PH04 (F-, Δ ((*argF-lac*)169, *lsrK*, *ptsH*) λ -) was constructed and cured previously. Restriction enzymes, Gibson master mix, and T4 ligase were purchased from New England Biolabs (Ipswitch, MA).

Plasmid Construction and Cloning. The plasmids listed in Table 1 were used in this publication. All plasmids are named using a general "Promoter/Inducer-general product" system; e.g., OxyR-sfGFP is named as such because it has sfGFP downstream of an OxyR-regulated oxyS promoter. AI-1tyrosine is named as such because AI-1 induces several genes involved in tyrosine biosynthesis. OxyR-LasI-LAA, 29 OxyRsfGFP,²⁹ AI-1-GFPmut3,³⁶ AI-1-tyrosine,³⁴ and pAHL-ptsH² were all constructed in previous publications. ZA-tyrosine was constructed by digesting AI-1-tyrosine with the enzymes KpnI-HF and EagI-HF and inserting the region containing aroG, aroE, and tyrA into vector the ZA31MCS after an uninhibited pLtet0-1 promoter using the existing *Kpn*I-HF site and a PCR added EagI-HF site. OxyR-LasI-LAA-GFPmut3 was constructed by inserting the RBS site and GFPmut3 gene from AI-1-GFPmut3 behind the LasI-LAA sequence using a Gibson reaction.

ORR Reaction in Biological Media. The ORR reaction was performed in biological media as described previously³⁷ in a chamber resembling the one depicted in Scheme 1. A standard gold-disk working electrode (2 mm diameter; CH Instruments, Austin, TX), a 4-in. platinum counter wire (Alfa Aesar; Havermill, MA), and a Ag/AgCl reference electrode (Bioanalytical Systems Inc.; West Lafayette, IN) were each placed in a 17 mm diameter glass vial using a fitted cap to create a standard 3-electrode cell with 1 mL of minimal media. All gold electrodes were precleaned first by polishing with 0.05 um diameter silicon polishing powder (CH Instruments) followed by 30 s incubation in a piranha solution of 7:3 ratio of 18.4 M sulfuric acid to 30% hydrogen peroxide. A small Teflon-coated stir bar was carefully added to both increase dissolved oxygen content and homogenize the solution. Using a CHI1040c electrochemical analyzer (CH Instruments), an IT procedure (i.e., Current vs Time) was run to apply a

constant voltage at -0.5 V vs Ag/AgCl while constantly measuring current. Solutions were then stored on ice and protected from light for later analysis. Electrodes were similarly tested for fouling caused by multiple uses by removing the media and replacing it with a fresh 1 mL sample. Hydrogen peroxide content was determined using a Pierce quantitative hydrogen peroxide assay (Thermo Fisher; Waltham, MA). Current and charge analysis was performed in Matlab R2020b (Mathworks; Natick, MA). Current waveforms were smoothed using Matlab's Smooth function to remove noise introduced from the stir bar.

ORR Electrogenetic Induction and Fluorescent Measurement. The ORR reaction was performed as described above however electrodes first underwent a post cleaning "passivation treatment" by running an IT-curve in cell-free minimal media for 1800 s. We found this dramatically reduced experiment-to-experiment variability. In monocultures, E. coli cells were kept to an OD_{600} of 0.1. In cocultures, transmitter and receiver cells were added at an OD_{600} of 0.005 and 0.1, respectively. Three separate 1 mL cultures were induced at a time using 3 separate electrochemical cells. After a particular test variant was finished, the samples were removed and returned to disposable culture tubes and the next sample was loaded into the electrochemical cells. Once all tests were completed, all culture tubes were moved to a 37 °C 250 rpm shaker for 3 h. GFPmut3 and sfGFP expression were measured using a Tecan Spark plate reader (Tecan Group Inc.; Männedorf, Switzerland) and a BD FACSCelesta flow cytometer (Becton, Dickinson, and Company; Franklin Lakes, NJ). Flow cytometry analysis was performed using FlowJo (FlowJo LLC; Ashland, OR). In flow cytometry analysis, the activated cell threshold gate was defined as fluorescence exceeding 2 standard deviations above the average of the null control. Positive controls were established using hydrogen peroxide and AI-1 added at various concentrations to monocultures.

Tyrosine and Coculture Composition Measurements. Tyrosine was measured using differential pulse voltammetry (DPV), a 3 mm glassy carbon working electrode, a 4-in. platinum counter wire, and a Ag/AgCl reference electrode. DPV waveform settings were the same as used previously for measuring clozapine,³⁸ except the voltage range (0.5–0.8 V vs Ag/AgCl). The peak current from these measurements were then compared to a standard curve prepared from measurements of known tyrosine concentrations. The percentage of the growth-regulated cells was calculated from dsRed fluorescence measurements in combination with a fluorescence vs optical density calibration curve made with known concentrations of cells.

RESULTS AND DISCUSSION

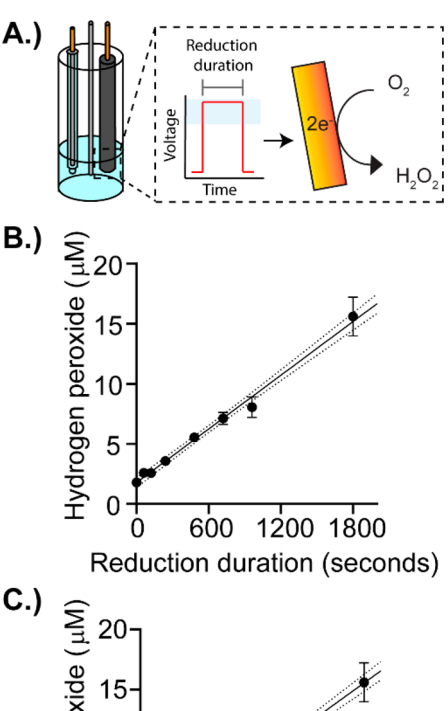
Electrode-Actuated Generation of Hydrogen Peroxide. We first characterized hydrogen peroxide formation by ORR in a variety of conditions, including in biological media. The ORR reaction involves the transfer of 2-electrons at an electrode surface to dissolved oxygen.³⁹ We focused on three main issues: the influence of pH, electrode fouling in biological media, and the relationship between charge transferred and hydrogen peroxide generated. To do this, we constructed a simple 3-electrode cell with a 2 mm diameter gold working electrode positioned just above a small stir bar in 1 mL of minimal media (see chamber depicted in Scheme 1).

An electrochemical analyzer was used to continuously bias the gold working electrode (ϖ -0.5 V vs Ag/AgCl). This voltage maximizes hydrogen peroxide generation while avoiding water reduction, which becomes more prevalent below -0.55 V vs Ag/AgCl.⁴⁰ Hydrogen peroxide was measured using a commercially available kit (see Methods). Results depicting pH-dependence and fouling are summarized in Figure S1A,B. Briefly, we found that ORR is more efficient at basic pH, as previously reported, 41 and produced sufficient peroxide at pH 7.5 (see Figure S1A) for subsequent cell-based experiments. Similarly, fouling only significantly occurred between the first and second uses of an electrode and was mitigated by a pre-experiment "passivation" treatment in minimal media (see Methods). We found passivated electrodes were repeatably biased generating the same amount peroxide over the course of at least 5 experiments (see Supporting Information, Figure S1B).

That is, to test the relationship between charge and hydrogen peroxide formation, we biased passivated electrodes in fresh media at constant voltage for different amounts of time. We then calculated the overall charge transferred and plotted the peroxide formation vs both charge and the duration of the applied charge. We observed linear relationships in both cases: (i) H₂O₂ vs input time (i.e., reduction duration) and (ii) H₂O₂ vs the total charge (see Figures 1B,C, respectively). We then calculated that the overall energy efficiency of the peroxide generation process (i.e., the number of electrons added to oxygen in the form of H2O2 divided by the number of electrons transferred into the liquid). We found this was approximately ~8% for all reduction durations greater than 60 s (Figure S1C). In sum, these results indicated that hydrogen peroxide was controllably propagated into the biological media by regulating the time over which we applied a -0.55 V vs Ag/ AgCl reductive potential.

Electrogenetic Activation of Green Fluorescent Protein (GFP). Next, we investigated the extent to which electrogenetic control could be propagated into a well-mixed monoculture using ORR-generated hydrogen peroxide. We used *E. coli* with an *oxyR-sf GFP* plasmid developed previously²⁹ to test whether increasing the duration of the ORR procedure (i.e., increasing H₂O₂ generated) would result in increasing activation of the *oxyS* promoter, thus resulting in increased sfGFP fluorescence (see Figure 2A).

In previous work on hydrogen peroxide-induced cell motility, 42 we found that we needed to balance $\rm H_2O_2$ concentration with cell number both to avoid toxicity and to ensure oxyR-mediated gene expression. Beyond toxicity and sufficiency for activating a genetic response, was the finding that $E.\ coli$ cells could rapidly consume/degrade hydrogen peroxide—even when 50 μM was added to cultures at $\rm OD_{600}$



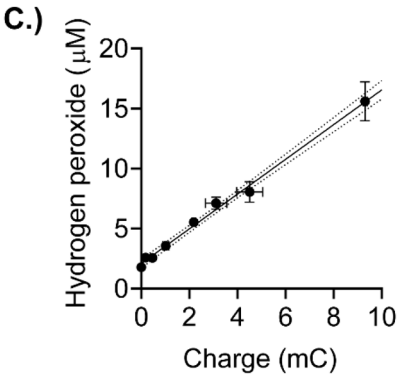


Figure 1. The 2-electron oxygen reduction reaction (ORR) produces hydrogen peroxide in biological media via a time-dependent electrochemical electron exchange. (A) The ORR reaction consumes dissolved oxygen to produce hydrogen peroxide using a reductively biased gold electrode. The major inputs are (i) the applied voltage and (ii) the duration of the applied voltage (i.e., the "reduction duration"). (B) When applying a constant voltage of $-0.5~\rm V~vs~Ag/AgCl$, the amount of hydrogen peroxide measured in the bulk media (stirred cell) was found to increase linearly with time. (C) Similarly, the hydrogen peroxide formed was found to be linearly correlated with the amount of charge transferred, indicating the electronic input is guiding the overall rate of the reaction in this particular electrochemical cell. Dotted lines represent 95% confidence interval of linear fits (n = 3).

 $\sim 0.1.^{43}$ That said, after mixing both transmitter and receiver cells together at fixed ratios and cell densities, we found that an initial OD₆₀₀ of 0.1 was optimal for generating GFP and for minimizing deleterious effects on growth (data not shown) in response to a range of hydrogen peroxide concentrations (typically less than 50 μ M). Then, using the same electrochemical cell as described above, we introduced cells into the ORR cell, biased the electrode to -0.5 V vs Ag/AgCl for specified times, and then followed cell growth and gene expression for 3 h in a 37 °C 250 rpm shaker. As anticipated, we found that increasing the reduction duration resulted in an increase in fluorescence, but interestingly the response was less than the fluorescent response of cells induced by a bolus of an equivalent hydrogen peroxide level (Figure 2B). Specifically, from Figure 1, we calculated the hypothetical concentration of H₂O₂ generated corresponding to a given duration and added

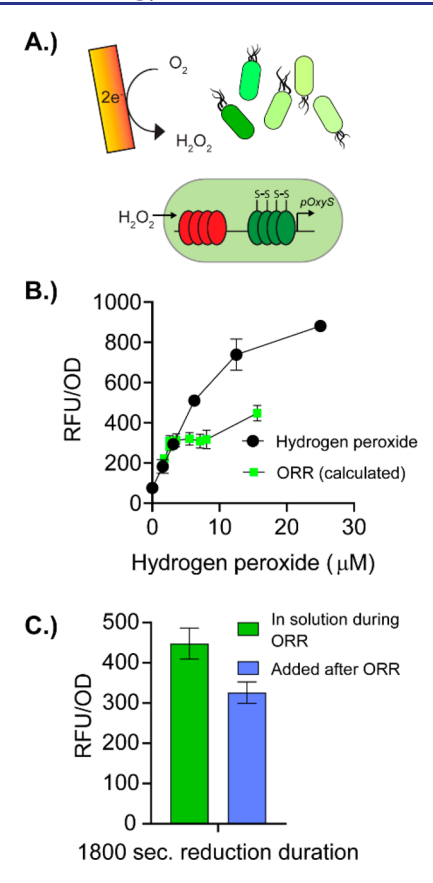


Figure 2. ORR induction of OxyR gene circuits is sensitive to transport limitations. (A) The ORR reaction occurs at the electrode surface and $\rm H_2O_2$ must diffuse into the bulk media. *E. coli*, however, rapidly degrades hydrogen peroxide creating a strong localized concentration gradient decreasing with distance away from the electrode. The end result is heterogeneous activation within the population. (B) Hydrogen peroxide induction via bolus (black) exceeded ORR induction (green) when eliciting a fluorescent response at equivalent concentrations. (C) When cells were added after the ORR reaction had completed, thus allowing the produced hydrogen peroxide to homogenize throughout the solution, the overall induction was lower, suggesting that the fluorescent response was subject to localized concentrations of hydrogen peroxide during the ORR formation.

this amount to uncharged cells. In Figure 2B, the cells supplemented with hydrogen peroxide generated far more GFP than those exposed to hydrogen peroxide generated at the electrode, particularly when added at levels exceeding 5 μ M. We hypothesized that these observations were due to either the degradation of hydrogen peroxide as a function of its distance away from the electrode surface or the transient nature by which cells would be induced near the electrode in corroboration with our prior work modeling hydrogen peroxide production and cellular degradation in a static media.²⁹ We note these induction methods are quite different. In the case of a bolus of hydrogen peroxide added to a stirred culture, the cells (or a fraction thereof) are exposed to a fairly uniform concentration.⁴⁴ In the case of the ORR-generated peroxide, its appearance occurs over time as well as its interactions with cells that are in the proximity of the electrode. Most notably, even in quiescent fluids, our modeling efforts showed that hydrogen peroxide generated in this manner accumulated to \sim 60 μ M at the electrode surface, but never accumulated beyond 5 mm away from the electrode owing in large part to its consumption. Our data here for the ORR generated $\mathrm{H_2O_2}$ are consistent with a situation wherein only cells that pass nearest the electrode during the reduction period would experience a concentration of peroxide sufficient to induce a strong genetic response. Other cells might experience a far lower concentration, if at all. As a result, both the per cell fluorescence would be lower and a significant fraction of cells would be poorly induced throughout the reduction process.

We ran an experiment to provide additional evidence for the heterogeneity associated with this induction method. Specifically, we cultivated cells in the presence of ORR run for the longest reduction duration (1800 s). In parallel, we ran the ORR reduction in fresh media for the same duration, but added the cells only after the reaction had completed. In this way, the peroxide generated would have fully equilibrated throughout the solution and reached a maximal level. Each group was then incubated for an additional 3 h and GFP expression was measured to assess oxyR induction. Interestingly, when cells were added after the peroxide had been fully generated, we found a *lower* overall fluorescence (Figure 2C). Previous modeling had similarly found that the hydrogen peroxide produced by ORR varies dramatically within 1 mm of the electrode surface and the gradient was further exasperated by the presence of cells.²⁹ These results similarly suggest there exist localized concentration gradients experienced by the cells during the ORR, and importantly, some cells actually experienced higher levels of H2O2 than the average (which would have been the case for the second culture).

Monoculture vs Transmitter/Receiver Signaling, To further evaluate whether there was heterogeneity in signal recognition, we characterized the same experiments using flow cytometry. We also conceived of and tested an information relay "transmitter-receiver" coculture model depicted in Figure 3A. In this later model, one cell population contains the plasmid OxyR-LasI-LAA, which produces the LasI bacterial autoinducer-1 synthase in response to hydrogen peroxide. The encoded LasI synthase, in effect, "transmits" information in the form of autoinducer-1 (i.e., N-3-oxododecanoyl homoserine lactone, abbreviated AI-1) from these "transmitter" cells based on their perception of the input hydrogen peroxide signal. This AI-1 molecule then serves as a second chemical messenger. As a native bacterial signaling molecule, AI-1 is not subject to rapid degradation or other surface-generated local effects. More importantly, the information conveyed by this second messenger is of a different form and the energy provided for its dissemination stems from the available nutrients. Moreover, it is not associated with a pathogen, wound, or oxidative stress alarm (as is H₂O₂), rather it is a principal form of bacterial cell-cell conversation and cues bacterial quorum sensing responses. QS signals are noted in that they provide for a collective response among a population of cells. 45 Incorporation of different information "types" is an advantage in a transmitter/receiver communication system in that it enhances the design space and offers increased opportunity to generate multiple genetic circuits having different functions. Here, a "receiver" population responds to the transmitted AI-1 signal through an AI-1 regulated genetic circuit (i.e., AI-1-GFPmut3) that can be monitored by measuring GFP fluorescence (Figure S2A). We found in preliminary tests that an initial ratio of 0.05 transmitter/receivers and an initial overall OD_{600} of 0.1 resulted in minimal uninduced activation within the receiver population, while preserving robust peroxide-dependent

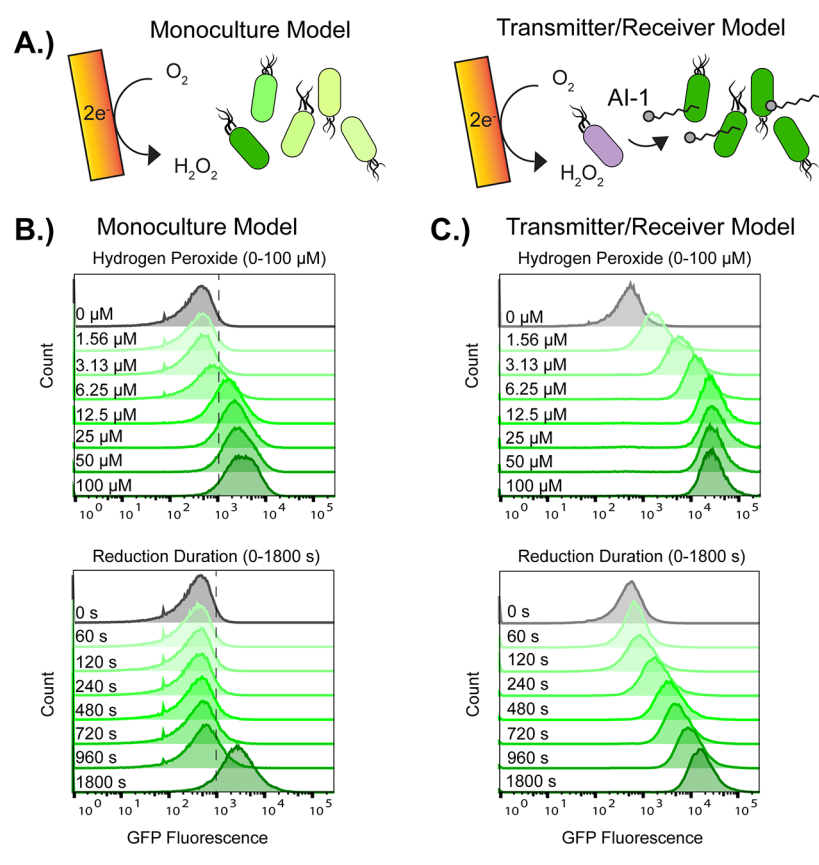


Figure 3. Information transfer through a transmitter/receiver coculture model yielded superior electrogenetic control via the ORR reaction. (A) Two models were proposed to analyze information transfer from the electrode to the culture: (i) a monoculture model (left) in which hydrogen peroxide induces GFP expression in a monoculture; (ii) a coculture model (right) in which hydrogen peroxide induces production of an AI-1 molecule by a "transmitter" population which in turn activates expression of GFP in a "receiver" population. We analyzed the monoculture model (B) and the transmitter/receiver model (C) for fluorescent activation using flow cytometry when adding hydrogen peroxide (middle panel) or when hydrogen peroxide was produced by ORR (bottom panel). Hydrogen peroxide induction in both models produced bell curves that shifted to the right in a uniform manner. ORR induction of the monoculture led to a right-shift of the leading edge of the bell curve (bottom left, see vertical line), while the coculture model saw the entire curve shift with each increased concentration (bottom right). 30 000 cells were measured in every histogram.

activation (Figure S2B). Importantly, we also saw that the fluorescent signal measured from the coculture seemed to saturate above 12.5 μ M hydrogen peroxide, which is near the upper limit of producible concentrations using our particular electrochemical cell (Figure 1B). This suggests that this ratio of transmitter to receiver cells ought to have a titratable expression level across the full range of electrochemical inputs.

In order to precisely compare the mono- and coculture communication modalities via FACS, we reran experiments with a monoculture of OxyR-LasI-LAA-GFPmut3 (OLG) using the ORR induction process. That is, in this case, the transmitter cells produce both the AHL synthase and GFP. Fluorescence measurements, therefore, directly reflect perception of the hydrogen peroxide and induction of the AHL synthase. In Figure 3B, we show results from experiments where either hydrogen peroxide was added at various concentrations (middle left panel) or the -0.5 V reducing potential was applied for various times (bottom left panel). The data depicted from samples taken 3 h after the charge was initially applied. We found that the induction of OLG cells in monoculture increased with hydrogen peroxide and reduction duration, but the increase caused by ORR induction was largely produced by a widening of GFP distribution (noted by the vertical line placed at the leading edge of the t₀ sample) or by a large shift (at 1800 s). In the end and in both cases, the mean GFP levels reached were $\sim\!2-4\times10^3$ RFU.

By comparison, in Figure 3C, we found that for the transmitter/receiver coculture model there was a monotonic increase in the distribution of GFP with hydrogen peroxide, irrespective of its mode of addition. Specifically, we observed a fairly rapid increase in GFP production at the lower levels of H₂O₂ addition that appeared to saturate at levels above 12.5 μ M. In the case where H₂O₂ was generated by an electrode, a steady increase in fluorescence was observed over all times. In the end, the extent of GFP expression (median level reached) was significantly greater ($\sim 1-3 \times 10^4$ RFU) than the monoculture model while simultaneously maintaining a lower robust coefficient of variation (Figure S3). These results indicate that the transmitter/receiver model resulted in greater gene expression with a lower variation in fluorescence activation. Interestingly, if one estimates the amount of H₂O₂ generated from our results in Figure 2, then for the 1800 s duration the level of H_2O_2 would have been 15 μ M in total, suggesting far less electronic energy was expended to achieve similar results. That is, a transmitter/receiver system that builds on cell recognition and dissemination also incorporates biological energy input (i.e., from other sources) and is typically extraordinarily efficient. We should also highlight here that the fraction of transmitter cells was initially ~5% and our

FACS data from 3 h later confirms that they did not accumulate as a dominant fraction.

In Figure 4A,B, we defined activation gates for each model system to analyze the percentage of induced cells in each case

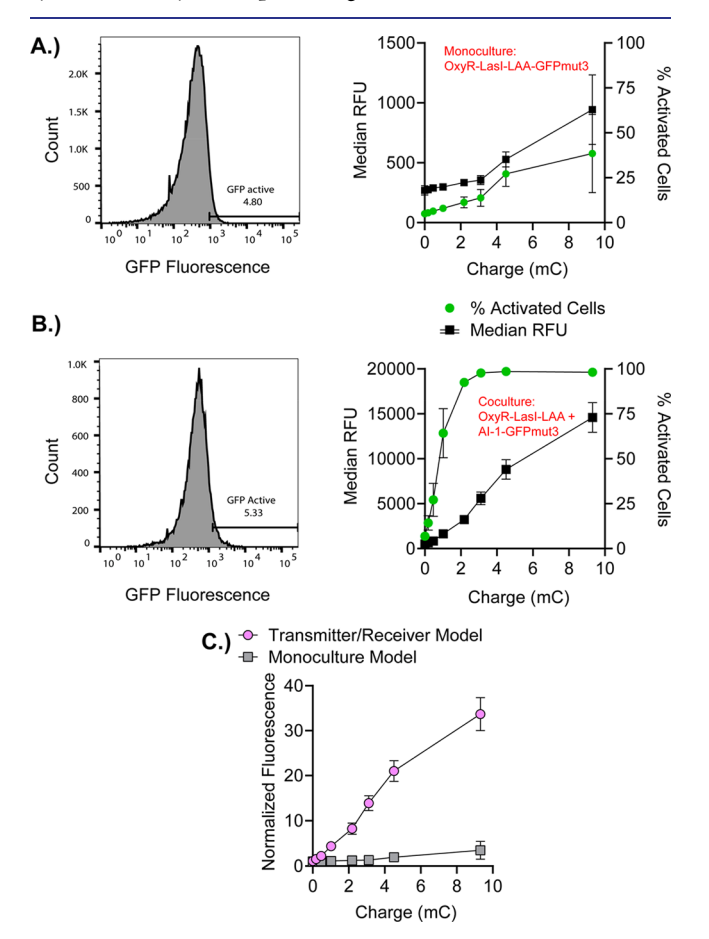


Figure 4. Coculture communication can relay electronically transmitted signals to homogenize the response of the overall culture. To analyze heterogeneous activation, for both the monoculture (A) and transmitter/receiver models (B), a fluorescent "activation" gate was defined such that any cell of greater that the ~95th percentile of the null control would be considered strongly induced. (A) Median fluorescent intensity (black) increased with reduction duration (i.e., charge) in the monoculture model; however, the average percentage of activated cells (green) remained low (<30%) over the full range of applied charge (1800 s duration). (B) Within the transmitter/receiver coculture model, both the median fluorescence (black) and the percent of activated cells (green) increased rapidly with increasing charge, indicating a homogeneous response. (C) The transmitter/ receiver model greatly outperformed the monoculture model, achieving a ~30 fold increase in gene expression across the charge levels tested. Values were normalized to their uninduced condition.

relative to the median fluorescence of the entire system (see Methods). The results of this gating (green dots, right axis) are shown in the right panel for both the monoculture (Figure 4A) and the coculture transmitter/receiver model (Figure 4B). The median fluorescence of the entire population is shown on the left axis (black dots). In the monoculture, the fraction that was activated reached 25% after 960 s of applied charge. Comparing the results at different reduction durations confirmed that the induction process was uneven across the population because the "activated" fraction remained low despite increases in the median RFU. Therefore, the increases

in fluorescent for the monoculture model were predominantly coming from a small-fraction of highly activated cells. Conversely, virtually 100% of the cells in the coculture were activated with less than 600 s of applied charge. Further, the mean fluorescence in the coculture was \sim 15-fold higher than the monoculture. Given that the monoculture model is a comparable indicator of transmitter activation within the coculture model, this indicates that the enhanced activation in the coculture occurs due to communication. This is evident by comparing the activation at 600 s reduction duration: the coculture model is 100% activated despite the monoculture model being less than 15% activated at the same input.

It is particularly interesting to directly compare the specific RFU values between the monoculture and the transmitter/ receiver cases (the transmitter/receiver fluorescence far exceeding that of the monocultures). That is, there is approximately 10-fold more GFP produced when the original electronic signal is translated into a chemical QS signal and propagated among the cells. Both the per cell expression level was increased as well as the total number of activated cells. In Figure 4C, we normalized the fluorescence data to the null control samples and plotted the resultant fluorescence data per cell as a function of the duration of our applied voltage. We found a roughly 30-fold increase in the case of the coculture signal propagation model, demonstrating even more clearly the benefit of transforming the initial electrochemical signal to a chemical second messenger as a means for controlling the coculture output.

Signal Propagation for Small Molecule Production. In order to demonstrate utility for electrogenetic actuation and biological signal propagation, we designed a coculture system wherein the receiver population makes a product of interest instead of a GFP marker. Further, we engineered two receiver strains that would synthesize and secrete the aromatic amino acid, tyrosine, as a result of receiving the AI-1 signal transmitted by the transmitter population. Additionally, to demonstrate the added design flexibility brought about by incorporating synthetic biology into signal propagation, we introduced two independent strategies for information transfer, both enabling tyrosine production (scheme in Figure 5A,B). In the first case, the well-studied tyrosine enzymatic synthesis pathway⁴⁶ is activated by the AI-1 signal through the induced expression of the aroG, aroE, and tyrA genes. In the other case, the identical pathway is present but constitutively expressed. In this case, we instead activate ptsH, the enzyme encoding HPr, a key component of hexose uptake in the PTS system. As a result, cells expressing the ptsH gene grow faster in response to an AI-1 signal forwarded by the transmitter population.² This results in increased metabolic activity and number of fastergrowing tyrosine-producing cells. In both cases, all cells (i.e., transmitter and receiver) were electronically induced as described earlier and then grown in a 37 °C, 250 rpm shaker for 24 h. We subsequently measured tyrosine using an electrochemical assay (Figure S4A,B). That is, at ~0.65 V vs Ag/AgCl the concentration of tyrosine is electronically measured from the peak current (see Methods).

In the case where we induced the pathway enzymes (Figure 5A), the tyrosine concentration increased concomitantly with reduction duration (from 0 to 900 s) with levels steadily increasing from ~0.04 to 0.08 g/L. This plateaued between 900 and 1800 s. These levels are consistent with our earlier work measuring AI-1 from pathogen samples using the same plasmid.³⁴ For the growth-regulated model (Figure 5B), we

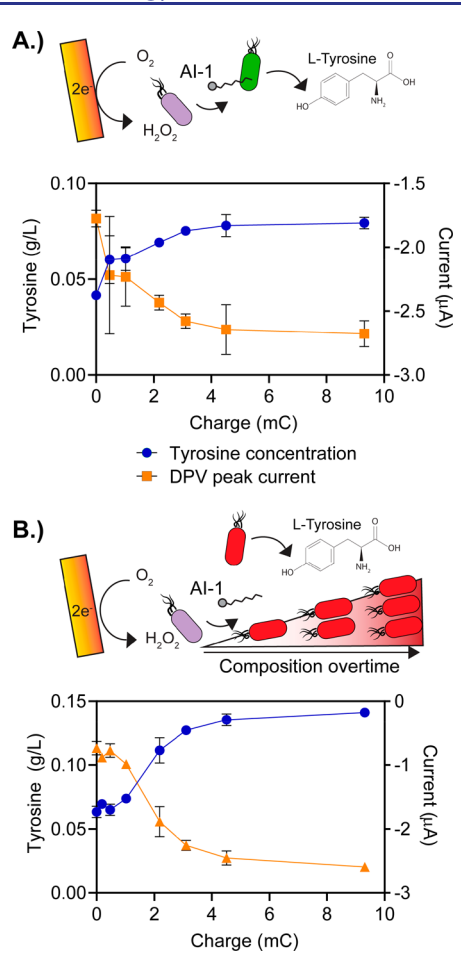


Figure 5. ORR electrogenetic control is well-suited both for controlling gene expression and for altering coculture composition during small molecule synthesis. (A) Using ORR to regulate transmission of an AI-1 signal, we found that an applied charge could be used to directly control the synthesis of tyrosine in an AI-1 sensitive producer strain. Here, tyrosine is measured electrochemically using differential pulse voltammetry (DPV), laying the framework for a full electrochemical feedback system. (B) Similarly, ORR could also be used to increase the growth rate of cells that constitutively produce tyrosine, thereby changing the overall composition of the batch culture. The end result was an increase in tyrosine concentration alongside concurrent increases in producer density (see Figure SS).

found that cells produced \sim 0.15 g/L tyrosine or about twice that of the pathway induced system. We should note that we have not optimized either system, but instead provide these as examples demonstrating the flexibility in developing synthetic biology constructs with different genetic circuits that in effect carry out the same overall function.

In this latter case, to test whether the increased tyrosine was attributed to the relative number of tyrosine producing cells, we modified the second population so that it would fluoresce red and also grow faster. Specifically, we performed an additional set of experiments wherein we constitutively expressed dsRed in addition to the aroG, aroE, and tyrA genes in the receiver cells. We first measured the fluorescence as a function of OD in these cells expressing dsRed after overnight induction with AI-1 (Figure SSA; see Methods). We found a linear result ($R^2 > 0.99$). Then, we carried out exactly analogous experiments as in Figure 5B and measured the total OD and fluorescence of the coculture. Using these numbers and the standard curve in Figure S4A, we calculated a rough

composition of dsRed-expressing tyrosine-producing cells as a function of reduction duration (Figure S5B). As anticipated, the resulting trends were nearly identical with the previous tyrosine measurements in Figure 5B. That is, we found that the amount of tyrosine produced per OD increased with composition and reduction duration (Figure S5C) but also that the amount of tyrosine produced per OD was roughly constant when adjusting the calculation to only use the cell density of the producer fraction (Figure S5D).

These two modes by which the original electronic signal is disseminated into the coculture demonstrates both the pros and cons of either directly regulating metabolic flux or instead, changing the proportion of cells within a coculture. More importantly, however, it shows how an electronic signal can be translated into a biological signal that, in turn, can be used in many ways by integrating with designs of synthetic biology. Direct regulation potentially has finer control if the promoter (i.e., transcriptional regulation) is titratable. But, this method may be more difficult to use for maximal output as a variety of factors, such as repressor expression, gene copy number, and metabolic burden might need to be optimized and this optimization might be altered when in mixed culture and in dynamically changing environments. Conversely, while it may be challenging to exert fine control over coculture composition, the total batch output might be more easily maximized relative to the output of a monoculture as cell growth perturbations might more easily accommodate internal flux distributions, as noted by the benefits of QS-based autoinduction systems.

These experiments further demonstrate the potential for an electrochemical control process in which electrogenetic signals can be used to increase genetic expression within a reactor, particularly when signals can be transformed and stably propagated. Finally, because we made tyrosine, one could use oxidative voltammetry to dynamically monitor product formation. While this is beyond the scope of the present work, we are currently investigating such an approach, including with other redox active outputs of receiver cells.²⁹

In summary, we have shown that redox electrogenetics can be used to stimulate and guide coculture production and composition. We found that both the information transfer and overall efficiency of signal transmission is high using the ORR reaction in a transmitter/receiver architecture. That is, while the information content transmitted from the original electrode was only 8% efficient (i.e., electrons absorbed by oxygen relative to transmitted electrons), the addition of transmitter cells that use available carbon and other nutrients serves to amplify and transform the original electrical signal into a second and more robust message that reduces losses from heterogeneous induction. As a result, we found the use of the transmitter/receiver coculture system enabled a ~30× greater range of control than was possible for the monoculture. These enhancements thereby enabled regulation of both metabolite production and coculture composition in a manner that would not be possible otherwise.

It is also noteworthy that our system takes partial advantage of lossy, noisy signal activation (i.e., here meaning localized signal presentation, uneven activation across the population, and signal sensitivity to stochastic effects⁴⁷). Specifically, the number of cells in the transmitter population that were induced by passing the electrode surface was essentially proportional to the reduction duration (i.e., increasing the time increases the probability a cell will pass close enough to the

electrode to become activated). From the perspective of the original input being the current associated with the applied voltage, noisy (or partial) activation can also be attributed to the relatively low conversion efficiency to hydrogen peroxide. Our estimates are that roughly $10^{9-10'}$ electrons were discharged into the solution that actually resulted in cell activation (actuated genetic circuit). This reduces even further the amount of original signal actually transmitted. Somewhat paradoxically, the consequence is this lossy, noisy electroactivation serves to fine-tune the population-level recruitment of transmitters. Then, because the transmitters emit QS signals that natively transition the receiver cells to a collective, the incorporation of a second messenger relay further fine-tunes the system-level response. Additionally, the propagation of the second messenger is enabled by available nutrients, not externally applied energy. By comparison, a lossless system that has the same number of electrons discharged—but with perfect catalytic formation of hydrogen peroxide and complete activation of the entire transmitter population-would not contain any intermediate population distributions of transmitter activation between the maximum and minimum signal inputs, and would therefore result in a step-function in receiver cell fluorescence. Our reflection on noise propagation is consistent with previous studies addressing how native cellular ensembles enhance communication capacity through stochastic and localized effects. 48 We suggest that our study represents a clear demonstration of the robust nature by which cocultures might prove useful to mitigate design constraints of individual cells (i.e., limited signal sensitivity and genetic responsiveness) through communication flow between specialized modules.²¹ Lastly, our general structure of signal propagation, from surface-based electronic to bulk biological, also shows how electrogenetic control schemes might naturally and efficiently fit within broader systems, such as those that rely on chemical inducers, like acylated homoserine lactones, originating and moving throughout a transport system from a variety of points of origin—in this case cells induced near the electrode surface.

In the future, we believe this methodology can be extremely effective at communicating with a variety of organisms simultaneously, as is common in the various microbial niches like the gut microbiome⁴⁹ or the rhizosphere.⁵⁰ Electrogenetic devices might be constructed for use in these environments enabling systemic changes to either natural and/or engineered microbial networks that extend far beyond the original signal source.⁵¹ Similarly, cocultures enable divisions of labor within biomanufacturing and they can result in robust coordination.⁵² We suggest these activities can easily be plugged into modular electronic-to-cell transmitter communication schemes.⁵³ Originating signals can reverberate throughout a system based upon the production or degradation of a variety of secondary messengers, each activating autonomous circuits of simple or more complex function (e.g., oscillators). 54,55 It is also possible, due to the spatial confinement of the electrochemically produced signal, to multiplex the response based upon the positions of a variety of transmitter cells. We believe these new types of devices will enable unique forms of biocontrol throughout therapeutic, remedial, and manufacturing land-

ASSOCIATED CONTENT

Supporting Information

The Supporting Information is available free of charge at https://pubs.acs.org/doi/10.1021/acssynbio.1c00522.

Figure S1 contains tests regarding the amount of hydrogen peroxide produced from our electrochemical cell when the pH is varied (A), the reaction is repeated without cleaning the electrode (B), and the faradaic efficiency of reduction (C); Figure S2 contains calibration curves of the GFP reporter cells when induced with 3-oxo-C12-HSL (A) and when induced in coculture through stimulation of the transmitter cells by hydrogen peroxide (B); Figure S3 reports the robust coefficient of variation for the flow cytometry distributions in Figure 3 and Figure 4; Figure S4 is the measurement of known concentrations of tyrosine using differential pulse voltammetry (A) and the analysis of peak voltage versus tyrosine concentration (B); Figure S5 contains the standard curve of dsRed fluorescence versus known densities of cells (A), the calculated percentage of dsRed cells in the coculture (B), the amount tyrosine produced (C), and the amount of tyrosine produced per dsRed cell (D) in the coculture reported in Figure 5B (PDF)

AUTHOR INFORMATION

Corresponding Author

William E. Bentley — Fischell Department of Bioengineering, University of Maryland, College Park, Maryland 20742, United States; Institute for Bioscience and Biotechnology Research and Fischell Institute for Biomedical Devices, University of Maryland, College Park, Maryland 20742, United States; orcid.org/0000-0002-4855-7866; Email: bentley@umd.edu

Authors

ı

Eric VanArsdale — Fischell Department of Bioengineering, University of Maryland, College Park, Maryland 20742, United States; Institute for Bioscience and Biotechnology Research and Fischell Institute for Biomedical Devices, University of Maryland, College Park, Maryland 20742, United States

Juliana Pitzer – Fischell Department of Bioengineering, University of Maryland, College Park, Maryland 20742, United States

Sally Wang — Fischell Department of Bioengineering, University of Maryland, College Park, Maryland 20742, United States; Institute for Bioscience and Biotechnology Research and Fischell Institute for Biomedical Devices, University of Maryland, College Park, Maryland 20742, United States

Kristina Stephens – Fischell Department of Bioengineering, University of Maryland, College Park, Maryland 20742, United States; Institute for Bioscience and Biotechnology Research and Fischell Institute for Biomedical Devices, University of Maryland, College Park, Maryland 20742, United States

Chen-yu Chen – Fischell Department of Bioengineering, University of Maryland, College Park, Maryland 20742, United States; Institute for Bioscience and Biotechnology Research and Fischell Institute for Biomedical Devices, University of Maryland, College Park, Maryland 20742, United States

Gregory F. Payne – Institute for Bioscience and Biotechnology Research and Fischell Institute for Biomedical Devices, University of Maryland, College Park, Maryland 20742, United States; orcid.org/0000-0001-6638-9459 Complete contact information is available at: https://pubs.acs.org/10.1021/acssynbio.1c00522

Author Contributions

Preparation of manuscript (EV, GP, WB); Performed experiments (EV, JP, SW, C-YC, KS); Research oversight (GP, WB).

Notes

The authors declare no competing financial interest.

ACKNOWLEDGMENTS

Financial support of this work was provided in part by the National Science Foundation (CBET#1932963, ECCS#1807604, CBET#1805274), the US Department of Energy (DOE BER#SCW1710), and the Defense Threat Reduction Agency (HDTRA1-19-1-0021).

REFERENCES

- (1) Antonovsky, N.; Gleizer, S.; Noor, E.; Zohar, Y.; Herz, E.; Barenholz, U.; Zelcbuch, L.; Amram, S.; Wides, A.; Tepper, N.; Davidi, D.; Bar-On, Y.; Bareia, T.; David; Shani, I.; Malitsky, S.; Jona, G.; Bar-Even, A.; Milo, R. Sugar Synthesis from CO2 in Escherichia coli. *Cell* **2016**, *166* (1), 115–125.
- (2) Stephens, K.; Pozo, M.; Tsao, C.-Y.; Hauk, P.; Bentley, W. E. Bacterial co-culture with cell signaling translator and growth controller modules for autonomously regulated culture composition. *Nat. Commun.* **2019**, *10* (1), 4129.
- (3) Gupta, A.; Reizman, I. M. B. B.; Reisch, C. R.; Prather, K. L. J. J. Dynamic regulation of metabolic flux in engineered bacteria using a pathway-independent quorum-sensing circuit. *Nat. Biotechnol.* **2017**, 35 (3), 273–279.
- (4) Callura, J. M.; Cantor, C. R.; Collins, J. J. Genetic switchboard for synthetic biology applications. *Proc. Natl. Acad. Sci. U. S. A.* **2012**, 109 (15), 5850–5855.
- (5) Kim, E. M.; Woo, H. M.; Tian, T.; Yilmaz, S.; Javidpour, P.; Keasling, J. D.; Lee, T. S. Autonomous control of metabolic state by a quorum sensing (QS)-mediated regulator for bisabolene production in engineered E. coli. *Metab. Eng.* **2017**, *44*, 325–336.
- (6) Krawczyk, K.; Xue, S.; Buchmann, P.; Charpin-El-Hamri, G.; Saxena, P.; Hussherr, M. D.; Shao, J.; Ye, H.; Xie, M.; Fussenegger, M. Electrogenetic cellular insulin release for real-time glycemic control in type 1 diabetic mice. *Science* **2020**, *368* (6494), 993–1001.
- (7) Cress, B. F.; Trantas, E. A.; Ververidis, F.; Linhardt, R. J.; Koffas, M. A. Sensitive cells: enabling tools for static and dynamic control of microbial metabolic pathways. *Curr. Opin. Biotechnol.* **2015**, *36*, 205–214.
- (8) Deisseroth, K. Optogenetics. Nat. Methods 2011, 8 (1), 26-29.
- (9) Yamaguchi, M.; Ito, A.; Ono, A.; Kawabe, Y.; Kamihira, M. Heat-Inducible Gene Expression System by Applying Alternating Magnetic Field to Magnetic Nanoparticles. ACS Synth. Biol. **2014**, 3 (5), 273–279.
- (10) Pouzet, S.; Banderas, A.; Le Bec, M.; Lautier, T.; Truan, G.; Hersen, P. The Promise of Optogenetics for Bioproduction: Dynamic Control Strategies and Scale-Up Instruments. *Bioengineering* **2020**, *7* (4), 151.
- (11) Milias-Argeitis, A.; Rullan, M.; Aoki, S. K.; Buchmann, P.; Khammash, M. Automated optogenetic feedback control for precise and robust regulation of gene expression and cell growth. *Nat. Commun.* **2016**, *7* (1), 12546.
- (12) Folcher, M.; Oesterle, S.; Zwicky, K.; Thekkottil, T.; Heymoz, J.; Hohmann, M.; Christen, M.; Daoud El-Baba, M.; Buchmann, P.; Fussenegger, M. Mind-controlled transgene expression by a wireless-powered optogenetic designer cell implant. *Nat. Commun.* **2014**, *5*, 1–11
- (13) Ye, H.; Baba, M. D. E.; Peng, R. W.; Fussenegger, M. A synthetic optogenetic transcription device enhances blood-glucose homeostasis in mice. *Science* **2011**, 332 (6037), 1565–1568.

- (14) Moros, M.; Idiago-López, J.; Asín, L.; Moreno-Antolín, E.; Beola, L.; Grazú, V.; Fratila, R. M.; Gutiérrez, L.; De La Fuente, J. M. Triggering antitumoural drug release and gene expression by magnetic hyperthermia. *Adv. Drug Delivery Rev.* **2019**, *138*, 326–343.
- (15) Zhang, H.; Pereira, B.; Li, Z.; Stephanopoulos, G. Engineering Escherichia coli coculture systems for the production of biochemical products. *Proc. Natl. Acad. Sci. U.S.A.* **2015**, *112* (27), 8266–71.
- (16) Wang, L.; York, S. W.; Ingram, L. O.; Shanmugam, K. T. Simultaneous fermentation of biomass-derived sugars to ethanol by a co-culture of an engineered Escherichia coli and Saccharomyces cerevisiae. *Bioresour. Technol.* **2019**, *273*, 269–276.
- (17) Flores, A. D.; Ayla, E. Z.; Nielsen, D. R.; Wang, X. Engineering a Synthetic, Catabolically Orthogonal Coculture System for Enhanced Conversion of Lignocellulose-Derived Sugars to Ethanol. *ACS Synth. Biol.* **2019**, *8* (5), 1089–1099.
- (18) Thuan, N. H.; Trung, N. T.; Cuong, N. X.; Van Cuong, D.; Van Quyen, D.; Malla, S. Escherichia coli modular coculture system for resveratrol glucosides production. *World J. Microbiol. Biotechnol.* **2018**, DOI: 10.1007/s11274-018-2458-z.
- (19) Li, Z.; Wang, X.; Zhang, H. Balancing the non-linear rosmarinic acid biosynthetic pathway by modular co-culture engineering. *Metabolic Engineering* **2019**, *54*, 1–11.
- (20) Niu, F.-X.; He, X.; Wu, Y.-Q.; Liu, J.-Z. Enhancing Production of Pinene in Escherichia coli by Using a Combination of Tolerance, Evolution, and Modular Co-culture Engineering. *Front. Microbiol.* **2018**, DOI: 10.3389/fmicb.2018.01623.
- (21) Suderman, R.; Bachman, J. A.; Smith, A.; Sorger, P. K.; Deeds, E. J. Fundamental trade-offs between information flow in single cells and cellular populations. *Proc. Natl. Acad. Sci. U. S. A.* **2017**, *114* (22), 5755–5760.
- (22) Guo, X.; Li, Z.; Wang, X.; Wang, J.; Chala, J.; Lu, Y.; Zhang, H. De novo phenol bioproduction from glucose using biosensor-assisted microbial coculture engineering. *Biotechnol. Bioeng.* **2019**, *116* (12), 3349–3359.
- (23) Dinh, C. V.; Chen, X.; Prather, K. L. J. Development of a Quorum-Sensing Based Circuit for Control of Coculture Population Composition in a Naringenin Production System. *ACS Synth. Biol.* **2020**, *9* (3), 590–597.
- (24) Goers, L.; Freemont, P.; Polizzi, K. M. Co-culture systems and technologies: taking synthetic biology to the next level. *Journal of The Royal Society Interface* **2014**, *11* (96), 20140065.
- (25) Rugbjerg, P.; Sarup-Lytzen, K.; Nagy, M.; Sommer, M. O. A. Synthetic addiction extends the productive life time of engineer-edEscherichia colipopulations. *Proc. Natl. Acad. Sci. U. S. A.* **2018**, *115* (10), 2347–2352.
- (26) Weber, W.; Luzi, S.; Karlsson, M.; Sanchez-Bustamante, C. D.; Frey, U.; Hierlemann, A.; Fussenegger, M. A synthetic mammalian electro-genetic transcription circuit. *Nucleic Acids Res.* **2008**, *37* (4), No. e33.
- (27) Tschirhart, T.; Kim, E.; McKay, R.; Ueda, H.; Wu, H.-C.; Pottash, A. E.; Zargar, A.; Negrete, A.; Shiloach, J.; Payne, G. F.; Bentley, W. E. Electronic control of gene expression and cell behaviour in Escherichia coli through redox signalling. *Nat. Commun.* 2017, 8 (1), 14030.
- (28) Bhokisham, N.; VanArsdale, E.; Stephens, K. T.; Hauk, P.; Payne, G. F.; Bentley, W. E. A redox-based electrogenetic CRISPR system to connect with and control biological information networks. *Nat. Commun.* **2020**, *11* (1), 2427.
- (29) Terrell, J. L.; Tschirhart, T.; Jahnke, J. P.; Stephens, K.; Liu, Y.; Dong, H.; Hurley, M. M.; Pozo, M.; McKay, R.; Tsao, C. Y.; Wu, H.-C.; Vora, G.; Payne, G. F.; Stratis-Cullum, D. N.; Bentley, W. E. Bioelectronic control of a microbial community using surface-assembled electrogenetic cells to route signals. *Nat. Nanotechnol.* 2021, 16, 688.
- (30) Kang, M.; Kim, E.; Chen, S.; Bentley, W. E.; Kelly, D. L.; Payne, G. F. Signal processing approach to probe chemical space for discriminating redox signatures. *Biosens. Bioelectron.* **2018**, *112*, 127–135.

- (31) Melchionna, M.; Fornasiero, P.; Prato, M. The Rise of Hydrogen Peroxide as the Main Product by Metal-Free Catalysis in Oxygen Reductions. *Adv. Mater.* **2019**, *31* (13), 1802920.
- (32) Jo, I.; Chung, I. Y.; Bae, H. W.; Kim, J. S.; Song, S.; Cho, Y. H.; Ha, N. C. Structural details of the OxyR peroxide-sensing mechanism. *Proc. Natl. Acad. Sci. U.S.A.* **2015**, *112* (20), 6443–6448.
- (33) Gustavsson, M.; Bäcklund, E.; Larsson, G. Optimisation of surface expression using the AIDA autotransporter. *Microb. Cell Fact.* **2011**, *10* (1), 72.
- (34) VanArsdale, E.; Hörnström, D.; Sjöberg, G.; Järbur, I.; Pitzer, J.; Payne, G. F.; van Maris, A. J. A.; Bentley, W. E. A Coculture Based Tyrosine-Tyrosinase Electrochemical Gene Circuit for Connecting Cellular Communication with Electronic Networks. *ACS Synth. Biol.* **2020**, *9* (5), 1117–1128.
- (35) Ha, J.-H.; Hauk, P.; Cho, K.; Eo, Y.; Ma, X.; Stephens, K.; Cha, S.; Jeong, M.; Suh, J.-Y.; Sintim, H. O.; Bentley, W. E.; Ryu, K.-S. Evidence of link between quorum sensing and sugar metabolism in Escherichia coli revealed via cocrystal structures of LsrK and HPr. *Sci. Adv.* **2018**, *4* (6), No. eaar7063.
- (36) Saeidi, N.; Wong, C. K.; Lo, T. M.; Nguyen, H. X.; Ling, H.; Leong, S. S. J.; Poh, C. L.; Chang, M. W. Engineering microbes to sense and eradicate Pseudomonas aeruginosa, a human pathogen. *Molecular Systems Biology* **2011**, *7* (1), 521–521.
- (37) Stephens, K.; Zakaria, F. R.; VanArsdale, E.; Payne, G. F.; Bentley, W. E. Electronic signals are electrogenetically relayed to control cell growth and co-culture composition. *Metabolic Engineering Communications* **2021**, *13*, No. e00176.
- (38) Kang, M.; Kim, E.; Winkler, T. E.; Banis, G.; Liu, Y.; Kitchen, C. A.; Kelly, D. L.; Ghodssi, R.; Payne, G. F. Reliable clinical serum analysis with reusable electrochemical sensor: Toward point-of-care measurement of the antipsychotic medication clozapine. *Biosens. Bioelectron.* 2017, 95, 55–59.
- (39) Kulkarni, A.; Siahrostami, S.; Patel, A.; Nørskov, J. K. Understanding Catalytic Activity Trends in the Oxygen Reduction Reaction. *Chem. Rev.* **2018**, *118* (5), 2302–2312.
- (40) Genshaw, M. A.; Damjanovic, A.; Bockris, J. O. M. Hydrogen peroxide formation in oxygen reduction at gold electrodes: I. Acid solution. *Journal of Electroanalytical Chemistry and Interfacial Electrochemistry* 1967, 15, 163–172.
- (41) Zurilla, R. W.; Sen, R. K.; Yeager, E. The Kinetics of the Oxygen Reduction Reaction on Gold in Alkaline Solution. *J. Electrochem. Soc.* **1978**, 125 (7), 1103–1109.
- (42) Virgile, C.; Hauk, P.; Wu, H.-C.; Shang, W.; Tsao, C.-Y.; Payne, G. F.; Bentley, W. E. Engineering bacterial motility towards hydrogen-peroxide. *PLoS One* **2018**, *13* (5), No. e0196999.
- (43) Virgile, C.; Hauk, P.; Wu, H. C.; Bentley, W. E. Plasmidencoded protein attenuates Escherichia coli swimming velocity and cell growth, not reprogrammed regulatory functions. *Biotechnol. Prog.* **2019**, 35 (3), No. e2778.
- (44) Servinsky, M. D.; Terrell, J. L.; Tsao, C. Y.; Wu, H. C.; Quan, D. N.; Zargar, A.; Allen, P. C.; Byrd, C. M.; Sund, C. J.; Bentley, W. E. Directed assembly of a bacterial quorum. *ISME Journal* **2016**, *10* (1), 158–169.
- (45) Hooshangi, S.; Bentley, W. E. From unicellular properties to multicellular behavior: bacteria quorum sensing circuitry and applications. *Curr. Opin. Biotechnol.* **2008**, *19* (6), 550–555.
- (46) Juminaga, D.; Baidoo, E. E. K. K.; Redding-Johanson, A. M.; Batth, T. S.; Burd, H.; Mukhopadhyay, A.; Petzold, C. J.; Keasling, J. D. Modular Engineering of l-Tyrosine Production in Escherichia coli. *Appl. Environ. Microbiol.* **2012**, 78 (1), 89–98.
- (47) Rhee, A.; Cheong, R.; Levchenko, A. The application of information theory to biochemical signaling systems. *Phys. Biol.* **2012**, 9 (4), 045011.
- (48) Ellison, D.; Mugler, A.; Brennan, M. D.; Lee, S. H.; Huebner, R. J.; Shamir, E. R.; Woo, L. A.; Kim, J.; Amar, P.; Nemenman, I.; Ewald, A. J.; Levchenko, A. Cell-cell communication enhances the capacity of cell ensembles to sense shallow gradients during morphogenesis. *Proc. Natl. Acad. Sci. U.S.A.* **2016**, *113* (6), E679–E688.

- (49) Riglar, D. T.; Giessen, T. W.; Baym, M.; Kerns, S. J.; Niederhuber, M. J.; Bronson, R. T.; Kotula, J. W.; Gerber, G. K.; Way, J. C.; Silver, P. A. Engineered bacteria can function in the mammalian gut long-term as live diagnostics of inflammation. *Nat. Biotechnol.* **2017**, *35* (7), 653–658.
- (50) Wallenstein, M. D. Managing and manipulating the rhizosphere microbiome for plant health: A systems approach. *Rhizosphere* **2017**, 3, 230–232.
- (51) VanArsdale, E.; Pitzer, J.; Payne, G. F.; Bentley, W. E. Redox Electrochemistry to Interrogate and Control Biomolecular Communication. *iScience* **2020**, 23 (9), 101545.
- (52) Zhang, H.; Wang, X. Modular co-culture engineering, a new approach for metabolic engineering. *Metabolic Engineering* **2016**, *37*, 114–121.
- (53) Wang, S.; Payne, G. F.; Bentley, W. E. Quorum Sensing Communication: Molecularly Connecting Cells, Their Neighbors, and Even Devices. *Annu. Rev. Chem. Biomol. Eng.* **2020**, *11* (1), 447–468
- (54) Stricker, J.; Cookson, S.; Bennett, M. R.; Mather, W. H.; Tsimring, L. S.; Hasty, J. A fast, robust and tunable synthetic gene oscillator. *Nature* **2008**, *456* (7221), 516–519.
- (55) Danino, T.; Mondragón-Palomino, O.; Tsimring, L.; Hasty, J. A synchronized quorum of genetic clocks. *Nature* **2010**, *463* (7279), 326–330.

